Analog VLSI-based Modeling of the Primate Oculomotor System

Timothy K. Horiuchi*and Christof Koch
Computation and Neural Systems Program
California Institute of Technology
Pasadena, CA, 91125

May 7, 1998

Abstract

One way to understand a neurobiological system is by building a simulacrum that replicates its behavior in real-time using similar constraints. Analog **V**ery **L**arge **S**cale **I**ntegrated (VLSI) electronic circuit technology provides such an enabling technology. We here describe a neuromorphic system that is part of a long-term effort to understand the primate oculomotor system. It requires both fast sensory processing as well as fast motor control to interact with the world. A one-dimensional hardware model of the primate eye has been built which simulates the physical dynamics of the biological system. It is driven by two different analog VLSI chips, one mimicking cortical visual processing for target selection and tracking and another modeling brainstem circuits that drive the eye muscles. Our oculomotor plant demonstrates both smooth pursuit movements, driven by a retinal velocity error signal, as well as saccadic eye movements, controlled by retinal position error, and can reproduce several behavioral, stimulation, lesion, and adaptation experiments performed on primates.

*Please address all correspondence to Timothy Horiuchi, currently at the Krieger Mind/Brain Institute, 338 Krieger Hall, Johns Hopkins University, 3400 N. Charles St., Baltimore, MD 21218 or email at timmer@jhu.edu.

1 Introduction

Using traditional software methods to model complex sensorimotor interactions is often difficult because most neural systems are composed of very large numbers of interconnected elements with non-linear characteristics and time constants that range over many orders of magnitude. Their mathematical behavior can rarely be solved analytically and simulations slow dramatically as the number of elements and their interconnections increase, especially in cases where capturing the details of fast dynamics is important. In addition, the interaction of neural systems with the physical world often requires simulating both the motor system in question and its environment which can be more difficult or time-consuming than simulating the model itself.

Mead (1989b, 1990) and others (Koch, 1989; Douglas et al., 1995) have argued persuasively that an alternative to numerical simulations on digital processors is the fabrication of electronic analogues of neurobiological systems. While parallel, analog computers have been used before to simulate retinal processing and other neural circuits (Fukushima et al., 1970), the rapid growth of the field of "synthetic neurobiology"—the attempt to understand neurobiology by building functional models—has been made possible by utilizing commercial chip fabrication processes which allows the integration of many hundred thousand transistors on a square centimeter of silicon. Designing massively-parallel sensory processing arrays on single chips is now practical. Much has happened in this field in the last eight or so years, producing a considerable number of new analog CMOS building blocks for implementing neural models. Local memory modification and storage (Hasler et

al., 1995; Diorio et al., 1997), redundant signal representations, and most recently, long-distance spike-based signaling (Boahen, 1997; Mortara, 1997; Kalayjian and Andreou, 1997; Elias, 1993) now form part of the designer's repertoire.

In this paper we review work in our laboratory using neuromorphic analog VLSI techniques to build an interactive, one-dimensional model of the primate oculomotor system. At present, the system consists of two chips: a visual attention-based, tracking chip and an oculomotor control chip. With the continued growth of this system we hope to explore the system-level consequences of design using neurobiological principles.

1.1 Analog VLSI Approaches for Neural Modeling

The two main arguments for modeling biological systems in analog VLSI are its high speed of information processing and the potential benefits of working within similar design constraints.

The human brain contains on the order of 10^{11} neurons; while no digital simulation that we know of attempts to simulate the brain of an entire organism (including any species of Nematode[1]), eventually such simulations will be desirable. Nearly all neural models are composed of fine-grained parallel-processing arrays and implementing such models on serial machines usually results in low simulation speeds orders of magnitude away from real-time. The investigation of sensorimotor systems is one example situation where the interaction with the real world must either be adequately simulated inside the computer, or the simulation must run quickly

[1] The most detailed simulation of C. Elegans, which has only 302 neurons, involves but 10% of the neurons (Niebur and Erdös, 1993).

enough to interface with a physical model. Typically, a sufficiently realistic simulation of the real world is impractical. Spike-based circuit modeling is another example where simulations can be particularly slow since large, fast swings in voltage are frequent. Additionally, mixing widely disparate time scales within the same simulation leads to stiff differential equations which are notoriously slow to solve (e.g., learning in spiking networks). Provided the analog VLSI circuitry can produce the proper level of detail and is configurable for the types of models under investigation, neuromorphic analog VLSI models deliver the speed desirable for large-scale, real-time simulations. Furthermore, augmenting the system to accomodate more neurobiological detail or expanding the size of the sensory array does not affect the speed of operation.

A second intriguing yet more controversial, argument for the usage of VLSI analogues to understand the brain revolves around the claim that certain constraints faced by the analog circuit designer are similar to the constraints faced by nervous systems during evolution and development.

When designing analog circuits to operate in the natural world, the circuit designer must operate within a set of powerful constraints: (1) power consumption, when considering mobile systems, is important; (2) the sensory input array must deal with physical signals whose amplitude can vary up to ten orders of magnitude; (3) component mismatch and noise limit the precision with which individual circuit components process and represent information; (4) since conventional VLSI circuits are essentially restricted to the surface of the silicon chip, there is a large cost associated with dense interconnection of processing units on a single chip.

All of these constraints also operate in nervous systems. For instance, the human brain, using 12 to 15 Watts of power[2] must have evolved under similar pressure to keep the total power consumed to a minimum (Laughlin et al, 1998; Sarpeshkar, 1997). Neurons must also solve the problems of mismatch, noise, and dynamic range. The wiring problem for the brain is severe and constrains wiring to relatively sparse interconnection. Although the general-computing paradigm at the heart of the digital computer implies that *in principle* all of these constraints could be implemented in software simulations, in practice they rarely are. The reasons for this are convenience and simulation speed alluded to above.

There are, of course, limitations of analog VLSI design which are not found in the biological substrate (such as the two-dimensional substrate, or the lack of a technology that would allow wires to grow and to extend connections similar to filopodia) and some constraints in the biological substrate which are not found in analog VLSI (such as low resistance wiring, viability throughout development, and evolutionary back-compatibility). By understanding the similarities and differences between biology and silicon technology and by utilizing them carefully, it is possible to both maintain the relevance of these circuits for biological modeling and gain insight into the solutions found by evolution.

1.2 Biological Eye Movements

Primate eye movements represent an excellent set of sensorimotor behaviors to study with analog VLSI for several reasons. From the motor control perspective,

[2]The same power budget as the Mars Sojourner!

the oculomotor system has a relatively simple musculature and there is extensive knowledge of the neural substrate driving it. Behaviorally, the primate eye shows a diversity of movements involving: saccades (quick, reorienting movements), the vestibulo-ocular reflex (an image-stabilizing movement driven by the head-velocity-sensitive semi-circular canals), the opto-kinetic reflex (an image-stabilizing movement driven by wide-field image motion), smooth pursuit (a smooth movement for stabilizing subregions of an image), and vergence (binocular movements to foveate a target with both eyes). The required complexity of visual processing ranges from coarse temporal-change detection (for triggering reflexive saccades) to accurate motion extraction from subregions of the visual field (for driving smooth pursuit) to much more sophisticated processes involving memory, attention, and perception. Perhaps the most attractive aspect of eye movements is that the input and output representations have been well explored and the purpose of eye movements is fairly clear.

Although the human eye has a field of view of about 170 degrees, we see best in the central one degree, or fovea, where the density of photoreceptors is the greatest. Our eyes are constantly moving to scrutinize objects in the world with the fovea. Since visual acuity rapidly declines if retinal slip exceeds 2-3 deg/sec (Westheimer and McKee, 1975), our smooth eye movements (VOR, OKR, and smooth pursuit) are concerned with stabilizing these images.

While the optokinetic reflex (OKR) uses whole-field visual motion to drive image-stabilizing eye movements, smooth pursuit eye movements are characterized by their use of subregions of the field of view. Smooth pursuit allows primates to

track small objects accurately even across patterned backgrounds. Interestingly, smooth pursuit eye movements are found only in primates.

While all of the eye movements discussed above are concerned with image-stabilization, much of our visual behavior involves scanning a scene, moving from one part of an image to another. Saccadic eye movements are employed for this purpose, moving the eyes very rapidly to place visual objects onto the fovea. Saccades are rapid, reaching peak velocities of 600 deg/sec in humans and last between 25 and 200 msec dependent upon the saccade amplitude. Although saccades are fast, they have a relatively long latency, requiring between 150 msec and 250 msec from the onset of a visual target to the beginning of the observed movement (Becker, 1989). These are the only conjugate eye movements that humans can generate as voluntary acts (Becker, 1989). We are able to trigger saccades to visual, auditory, memorized, or even imagined targets.

2 A One-Dimensional Oculomotor Plant

In this section we describe the construction and performance of our one-dimensional oculomotor plant and the architecture of the analog VLSI chip which controls the motors for both saccadic and smooth pursuit eye movements.

2.1 The Physical Plant

The primate eye is driven by three sets of muscles: the horizontal, vertical, and oblique muscles. These muscles and other suspensory tissues hold the eye in its socket, producing mechanical dynamics with which the control circuits in the brain-

stem must contend. Both the muscles and the suspensory tissues are elastic and, in the absence of motorneuron activation, will return the orb to a forward-facing position; both also provide significant viscosity, producing an over-damped, spring–mass system.

While many different models of the oculomotor plant have been proposed to describe the physical dynamics (e.g., Westheimer, 1954; Robinson, 1964), a linear, second-order model of the form:

$$\frac{\theta(s)}{T_{ext}(s)} = \frac{1}{(1+s\alpha_1)(1+s\alpha_2)} \tag{1}$$

$$\alpha_1, \alpha_2 = \frac{m}{2I} \pm \frac{1}{2I}\sqrt{m^2 - 4kI} \tag{2}$$

has been the most widely used. In the equation above, k is the spring-constant, m is the damping coefficient, I is the rotational inertia, $\theta(s)$ represents the gaze angle and $T_{ext}(s)$ represents the externally-applied torque. The measured dominant time constant in the eye has been found to be approximately 250 msec (Robinson 1964; Keller, 1973). The force-length relationship of the eye muscles was first measured by Collins et al. (1975) by recording the agonist muscle tension required to hold the eye at different eye positions. While this relationship was fit well with a parabolic function, the combination of forces from both muscles tends to cancel the non-linearity, producing a more-or-less linear force–position relationship.

The oculomotor plant model we have constructed is a one degree-of-freedom turntable (Fig. 1) which is driven by a pair of antagonistically-pulling DC (direct-current) motors. The DC motors are used to generate torque on the eye by creating

tension on the ends of a thread attached at its center to the front of the turntable. The viscoelastic properties of the oculomotor plant are simulated electronically by measuring the angle and angular velocity of the eye and driving the motors to generate the appropriate torques on the eye. This allows the demonstration of the viscoelastic mechanical properties by directly manipulating the mechanical system. Because the biological dynamics are not too far from linear (Collins et al., 1975), the system's dynamics have been modeled as linear to simplify analysis and construction.

In the biological system, the fixation position is determined by the balance point of the agonist muscle tension and the passive elastic forces of all the muscle and suspensory tissues. In the hardware model, however, the two motors are not driven directly against each other (with one motor simulating the active muscle and the other motor simulating the combined elastic forces), rather the calculated difference in forces is applied to only one motor. This type of differential drive avoids the increased motor-bearing friction resulting from driving the two motors directly against each other. In addition to the primary motor signals, a small, tonic drive on both motors prevents slack in the thread from building up.

2.2 The Saccadic Burst Generator and Neural Integrator

To drive the oculomotor plant described in the previous section, the brainstem control circuitry must provide the proper signals to overcome both tissue elasticity and viscosity. In order to maintain fixation away from the center position, a sustained pulling force must be generated. Also, to complete an eye movement faster

than the eye's natural time constant, a large, transient, acceleration force must be generated. (Robinson, 1973) Both the transient and sustained component signals can be found in brainstem areas which drive the motorneuron pools (Strassman et al., 1986; Godaux and Cheron, 1996). Accurate balancing of these two component signals is necessary and is observed in the motorneurons driving the eye muscles. If the transient component is too large, the eye will overshoot the target position and the eye will drift backwards to equilibrium; if the transient is too small, the eye undershoots the target and the eye drifts onward to equilibrium after the saccade.

To generate these oculomotor control signals, we have designed an analog VLSI circuit (see Figure 2), based on models by Jürgens et al. (1981), McKenzie and Lisberger (1986), and Nichols and Sparks (1995), consisting of three main parts: the saccadic burst generator (which converts desired eye displacement to a velocity signal), the neural integrator (which integrates velocity signals to position signals), and the smooth pursuit integrator (which integrates acceleration signals to velocity signals). For saccadic eye movements, only the first two are utilized. The saccadic burst integrator is used to control the burst duration and the neural integrator holds a dynamic memory of the current eye position. This model uses initial motor error (the difference in position from the current gaze angle and the desired gaze angle) as the input to the system. Motor error represents the desired saccade vector which is easily derived from the retinal position of target, relative to the fovea.

Figure 2 shows the block diagram of the oculomotor control circuitry. The input signal to the burst generator is a voltage, Vin, specifying the amplitude and direction of the saccade. This signal is held constant for the duration of the saccade. The

model generates two signals: a transient pulse of spiking activity (Fig. 3A, signal A) and a step (signal B) of spiking activity, are combined as input to the motor units (signal C). A pair of these transient/step signals drive the two motors of the eye.

Saccades are coordinated in this model by a "pause" system (not shown) which inhibits the burst generator until a trigger stimulus is provided. The trigger stimulus also activates a sample-and-hold circuit which holds Vin constant throughout the saccade. During a saccade, the input, Vin, is continuously compared to the output of the burst integrator which integrates the burst unit's spike train. The burst neuron keeps emitting spikes until the difference is zero. This arrangement has the effect of firing a number of spikes proportional to the initial value of motor error, consistent with the behavior of short-lead burst neurons found in the saccade-related areas of the brainstem (Hepp et al., 1989). In the circuit, the burst integrator is implemented by electrical charge accumulating on a 1.9 pF capacitor. After the burst is over, the burst (or eye-displacement) integrator is reset to zero by the "pause" circuitry. This burst of spikes serves to drive the eye rapidly against the viscosity.

The burst of activity is also integrated by the neural integrator (converting velocity commands to changes in eye position) which holds the local estimate of the current eye position from which the tonic signal is generated. The neural integrator provides two output spike trains that drive the left and right sustained components of the motor command. The motor units receive inputs from both the saccadic burst units and the neural integrator and compute the sum of these two signals. Fig. 3A,

signal C shows output data from the burst generator chip which is qualitatively similar to spike trains seen in the motor neurons of the abducens nucleus of the rhesus monkey (Fig. 3B, King et al., 1986).

In addition to the saccadic burst generation circuitry, external inputs have been included to allow the smooth pursuit system to drive the eye motors through the common motor output pathway. This input and its use in smooth pursuit will be discussed in section 3.3.

2.3 Performance

By connecting the motor outputs to the oculomotor plant, saccadic eye movements can be generated. For testing purposes, all of the saccadic eye movements in this section were specified by an external signal. In section 3, saccades were guided by stimuli presented to a 1-D visual tracking chip mounted on the eye.

Fig. 3A shows an example of a saccade with its underlying control signals and Fig. 4A shows an overlay of 20 saccadic trajectories. Figure 4B shows the peak velocity of these 20 saccades as a function of the commanded saccade amplitude. Similar to the peak-velocity vs. amplitude relationship in primate saccades, the peak velocity increases for increasing saccade amplitude and then saturates. As the peak velocity of the saccades saturate, the duration of the saccades begins to increase linearly with amplitude. This saturation is due to the saturating transfer function in the burst unit. These characteristics are qualitatively consistent with primate saccades (Becker, 1989).

2.4 Adaptation of Post-Saccadic Drift

Through repeated experience in the world, nearly all animals modify their behavior on the basis of some type of memory. The ability to adapt and learn is not simply an added feature of neural systems, it is a fundamental mechanism which drives the development of the brain and may explain much about the structures and representations that it uses to compute. For this reason, we are beginning to explore the use of adaptation in our oculomotor system. While there are many different forms of adaptation and learning in the saccadic system, we focus on a particular form that has been implemented in our system.

In the generation of saccades, the sustained (or tonic) component of the command determines the final eye position while the ideal transient (or burst) component should bring the eye to exactly that position by the end of the burst. Mismatch of the burst and tonic components leads to either forwards or backwards drift following an undershoot or overshoot of the final eye position, known as *post-saccadic drift*. Studies in both humans and monkeys show that, in the case of muscle weakening or nerve damage which produces systematic undershooting of saccades, post- saccadic drift can be compensated for by some type of adaptation process which have time constants on the order of 1.5 days (Optican and Robinson, 1980). Ablation studies have further shown that control of the burst and tonic gains is independent and that their control depends on different areas of the cerebellum. In addition, retinal slip was shown to be a necessary and sufficient stimulus to elicit these adaptive changes (Optican and Miles, 1985).

To implement the memory structure for the burst gain in our burst generator, we

have utilized a relatively new "floating-gate" structure which combines non-volatile memory and computation into a single transistor. Floating-gate structures in VLSI (a MOS transistor gate completely insulated from the circuitry by silicon dioxide) offer extremely effective analog parameter storage with retention measured in years. Until recently, however, the use of floating-gates required the use of either ultra-violet (UV) radiation (Glasser, 1985; Mead, 1989a; Kerns, 1993) or bi-directional tunneling processes (Carley, 1989; Lande et al., 1996) to modify the charge on the floating node, both of which have significant drawbacks. The recent development of a complementary strategy of tunneling and hot-electron injection (Hasler et al., 1995; Diorio et al., 1995) in a commercially-available BiCMOS process has alleviated some of these difficulties. Adding and removing electrons from the floating-gate can be performed at extremely low rates, making it possible to create long training time constants.

To demonstrate the ability to reduce post-saccadic drift in our VLSI system, a sensitive direction-selective motion detector chip (Horiuchi and Koch, 1996) was mounted on the one-dimensional eye and motion information was read from the chip 100 msec after the end of the saccadic burst activity. The burst activity period (lower trace in Figs. 5A and 5B) is detected by reading a signal on the burst generator chip representing the suppression of the pause circuitry. A standard leftward saccade amplitude of about 23 degrees was programmed into the burst generator input and a saccade was repeatedly triggered. The motion sensor was facing a stationary stripe stimulus which would elicit a motion signal during and after the saccade burst.

The direction-of-motion information was summed across the motion detector array and a simple, fixed-learning-rate algorithm was used to determine whether to increase or decrease the gain. One hundred msec after each trial saccade, the motion detector output current was compared against two threshold values. If the output value was greater than the rightward motion threshold, indicating overshoot, a unit hot-electron injection pulse was issued which would reduce the floating-gate voltage and thus reduce the burst gain. If the integrated value was less than the leftward motion threshold, indicating undershoot, a unit tunneling pulse was issued which would increase the floating-gate voltage and thus increase the pulse gain.

Fig. 5A shows an experiment where the pulse gain was initialized to zero. With the particular learning rates used, eight trials were required before the gain was raised sufficiently to eliminate the post-saccadic drift. Fig. 5B shows a similar experiment where the pulse gain was initialized to a large value. In this case, within 41 trials, the pulse gain was lowered sufficiently to eliminate the post-saccadic drift. The learning rates used in this example were arbitrary and can be set over many orders of magnitude.

2.5 Triggering the Saccade

Although the saccadic eye movements presented thus far were manually triggered for testing purposes, the system has also been extensively used with visual input to close the sensorimotor loop. In the initial stages of this project, visual input was provided to the saccadic system in the form of a simplified analog VLSI model of the retino-collicular visual pathway. This enabled the system to trigger orienting saccades

to temporally-changing visual stimuli (Horiuchi et al., 1994). This visually-driven chip computed the centroid of temporal activity in one-dimension and triggered saccades when the sum of all the temporal-derivative signals on the array exceeded a threshold.

In other work, we have also triggered saccades to auditory targets using an analog VLSI model of auditory localization based on the barn owl auditory localization system (Horiuchi, 1995). Auditory saccades are interesting because sounds are most easily localized in the head-based coordinate frame, but eye movements (at the level of the saccadic burst generator) are specified in essentially retinotopic coordinates. A coordinate transform which compensates for different starting eye positions must be performed to correctly specify saccades to auditory targets.

3 Smooth Pursuit Eye Movements

While the saccadic system provides the primate with an effective alerting and orienting system to place targets in the fovea, in many cases, smooth tracking of objects may be desirable to retain the high visual acuity of the fovea. While the ability to move the eyes smoothly to stabilize wide-field visual motion is fairly universal, the ability to select only a portion of the visual field to stabilize is only highly developed in primates. To accomplish this task, some mechanism is needed to define where the object is and from what part of the scene to extract motion information.

3.1 Visual Attention and Eye Movements

A number of studies have revealed the involvement of selective visual attention in the generation of both saccadic (Kowler et al., 1995; Hoffman and Subramaniam, 1995; Rafal et al., 1989; Shimojo et al., 1995) and smooth pursuit eye movements (Khurana and Kowler, 1987; Ferrera and Lisberger, 1995; Tam and Ono, 1994). Attentional enhancement occurs at the target location just before a saccade as well as at the target location during smooth pursuit. In the case of saccades, attempts to dissociate attention from the target location disrupts their accuracy and latency (Hoffman and Subramaniam, 1995). It has been proposed that attention is involved in programming the next saccade by highlighting the target location. For smooth pursuit—driven by visual motion in a negative feedback loop (Rashbass, 1961)—spatial attention is thought to be involved in the extraction of the target's motion. Since the cortical, motion-sensitive, middle temporal area (MT) and the middle superior temporal area (MST) have been strongly implicated in supplying visual motion information for pursuit by anatomical, lesion and velocity-tuning studies, (see Lisberger et al., 1987 for review) a mechanism to selectively use the activity from the neurons associated with the target at the correct time and place is actively being sought. The modulation of neural activity in these areas, for conditions that differ only by their instructions, has been investigated. Although only small differences in activity have been found in areas MT and MST during the initiation of smooth pursuit towards a target in the presence of a distractor (Ferrera and Lisberger, 1997), strong modulation of activity in MT and MST has been observed during an attentional task to discriminate between target and distractor motions

(Treue and Maunsell, 1996).

Koch and Ullman (1985) proposed a model of attentional selection based on the output of a single *saliency map* by combining the activity of elementary feature maps in a topographic manner. The most salient locations are where activity from many different feature maps coincide, or at locations where activity from a preferentially-weighted feature map, such as temporal change, occurs. A winner-take-all (WTA) mechanism, acting as the center of the attentional "spotlight," selects the location with the highest saliency. While the WTA mechanism captures the idea of attending a single point-target, many experiments have demonstrated weighted vector-averaging in both saccadic and smooth pursuit behavior (Lisberger and Ferrera, 1997; Groh et al, 1997; Watamaniuk and Heinen, 1994). Analog circuits that can account for this diversity of responses (that is, vector averaging, winner-take-all, vector summation) need to be investigated.

3.2 An Attentional Tracking Chip

We have built an analog VLSI visual processing chip to select "salient" points in an image based on the winner-take-all model of attentional selection. Building on the work of Morris and DeWeerth (1996) on modeling selective visual attention, this chip incorporates focal-plane processing to compute image saliency and to select a target feature for tracking. The target position and the direction of motion are reported as the target moves across the array, providing control signals for tracking eye movements.

The computational goal of the attentional tracking chip is the selection of a sin-

gle target and the extraction of its retinal position and direction of motion. Figure 6 shows a block diagram of this computation. The first few upper stages of processing compute the saliency map from simple feature maps which drive the WTA-based selection of a target to track. Adaptive photoreceptor circuits (Delbrück 1993) (at the top of Fig. 6) transduce the incoming pattern of light into an array of voltages. The temporal (TD) and spatial (SD) derivatives are computed from these voltages and used to generate the saliency map and direction of motion. The saliency map is formed by summing the absolute-value of each derivative (|TD| + |SD|). The direction-of-motion (DM) circuit computes a normalized product of the two derivatives: $\frac{TD \cdot SD}{|TD|+|SD|}$. Fig. 7 shows an example stimulus and the computed features.

Only circuits at the WTA-selected location send information off-chip. These signals include: the retinal position, the direction-of-motion, and the type of target being tracked. The saccadic system uses the position information to foveate the target and the smooth pursuit system uses the motion information to match the speed of the target. The target's retinal position is reported by the position-to-voltage (P2V) circuit (DeWeerth, 1992) by driving the common position-output line to a voltage representing its position in the array. The direction of motion is reported by a steering circuit that puts the local DM circuit's current onto the common motion-output line. The saccadic triggering (ST) circuit indicates whether the position of the target warrants a recentering saccade based on the distance of the target from the center of the array. This acceptance "window" is externally specified.

Figure 8 shows the response of the chip to a swinging edge stimulus. The

direction of motion of the target (DM, upper trace) and the position of the target (P2V, lower trace) are displayed. As the target moves across the array, different direction-of-motion circuit outputs are switched onto the common output line. This switching is the primary cause of the noise seen on the motion output trace. At the end of the trace, the target slipped off the photoreceptor array and the winning-status jumped to a pixel centered on a small, stationary background begin.

3.3 Visually-Guided Tracking Eye Movements

To demonstrate smooth pursuit behavior in our one-dimensional system, we mounted the attentional tracking chip on the oculomotor system and used its visual processing outputs to drive both smooth pursuit and saccadic eye movements.

The motor component of the model used to drive smooth pursuit is based on a leaky integrator model described by McKenzie and Lisberger (1986) using only the target velocity input. Because retinal motion of the target serves as an eye-velocity error, direction-of-motion signals from the tracking chip are used as an eye acceleration command. Visual motion is thus temporally integrated to an eye velocity command and drives the oculomotor plant in parallel with the saccadic burst generator (Fig. 2).

To implement the smooth pursuit integrator in this system, off-chip circuits were constructed. The direction-of-motion signal from the tracking chip was split into leftward and rightward motion channels and used as eye acceleration commands which were integrated to eye velocity commands by the pursuit integrators (Fig 2). The integrator leak time constants were set to about 1 sec.

Oscillation in the pursuit velocity around the target velocity (at around 6 Hz) is a common occurrence in primates (upper trace, Fig. 10B) and is also seen in our system (but at about 4 Hz). Oscillations in this negative feedback system can occur from delays in visual processing and from large gain in the smooth pursuit integration stage. Our system has very little motion processing delay, but the gain on the integrator is large. Goldreich et al. (1992) have shown that in the primate system, visual motion delays appear to be the dominant cause of this oscillation.

When humans view natural scenes mixed with both stationary and moving objects, saccades and smooth pursuit are combined in an attempt to quickly take in a scene and scrutinize moving objects. How these two eye movements are behaviorally combined is still unclear. When humans or monkeys pursue fast, sinusoidally moving targets, the smooth pursuit eye movement becomes punctuated with catch-up saccades as the target speed exceeds the maximum pursuit speed and a retinal error builds up.

While visual motion provides the largest contribution to eye acceleration during the initiation and maintenance of pursuit, the target's retinal position and acceleration also contribute to driving the eye (Morris and Lisberger, 1985). In our hardware model, however, the pursuit system is driven by only the retinal velocity error. The saccadic system—dedicated to keeping targets near the center of the imager—uses position error to trigger and guide saccades. While these two motor control systems operate essentially independently, the visual target motion induced by the saccade must be suppressed at the input of the smooth pursuit integrator to prevent conflict between the two systems and to maintain the smooth pursuit eye

velocity across saccades.

Figure 9B exemplifies the integration of saccadic with smooth pursuit eye movements during the tracking of a sinusoidally swinging target. When the velocity of the target exceeds the peak velocity of the pursuit system, the target slips out of the central region of the chip's field of view and saccades are triggered to recenter the target.

In another experiment we used a step-ramp stimulus to illustrate the separation of the saccadic and smooth pursuit systems, activating both systems at once but in different directions. In primates, visually-triggered saccades (not including express saccades) have latencies from 150 to 250 msec, while the pursuit system has a shorter latency from 80 to 130 msec. With this stimulus, the pursuit system begins to move the eye in the direction of target motion before the saccade occurs (Lisberger et al., 1987). As there is no explicit delay in the current saccadic triggering system, an artificial 100 msec delay was added in the saccadic trigger to mimic this behavior (Fig. 10A). The latency of the model pursuit system without adding additional delays is approximately 50 to 60 msec. Fig. 10B shows comparison data from a step- ramp experiment in a macaque monkey.

4 Conclusions

The two-chip primate oculomotor system model presented in this paper is part of an on-going exploration into the issues of systems-level neurobiological modeling using neuromorphic analog VLSI. This work focuses on feedback systems which involve

sensory and motor interaction with natural environments. Within the analog VLSI framework, it has touched on various examples of sensorimotor control, learning, and the coordination of different eye movements. Saccadic and smooth pursuit eye movements have been integrated in the system, which has raised many questions about how to model their interaction. Adaptation of saccadic parameters based on biologically-constrained error measures has been demonstrated. The use of a simple winner-take-all model of visual attention for target selection and selective motion extraction has been demonstrated, raising many questions about the interaction between reflexive (collicular) and volitional (cortical) eye movement systems. Our ongoing work seeks to address many of these questions.

The main contribution of our work has been the demonstration of a real-time modeling system that brings together many different neural models to solve real-world tasks. To date, there are no other oculomotor modeling systems that use realistic burst generator circuits to drive an analog oculomotor plant with similar dynamics to the biological system. While other research groups have built biologically-inspired, visual tracking systems, the problems they encounter are generally not similar to the problems faced by biological systems because they do not solve the task with hardware that has similar properties. By building circuits which compute with the representations of information found in the brain, the modeling system presented here is capable of replicating many of the behavioral, lesion, stimulation, and adaptation experiments performed on the primate oculomotor system. Armed with a continuously growing arsenal of circuits, we will be emulating much larger and more realistic sensorimotor systems in the future.

Acknowledgements:

The authors thank Brooks Bishofberger for mechanical design of the oculomotor system and fabrication of some of the dynamics simulation electronics, Tobi Delbrück for advice on photoreceptor circuit layout, Paul Hasler for advice on the floating-gate structures, Tonia Morris and Steven P. DeWeerth for their assistance and guidance in some important parts of the attentional selection circuits. We would also like to thank Steven Lisberger, Rodney Douglas, and Terry Sejnowski for advice rendered over many years. The research reported here was supported by the Office of Naval Research (ONR) and the Center for Neuromorphic Systems Engineering as part of the National Science Foundation Engineering Research Center Program.

References

Becker, W. (1989). Metrics. In Wurtz, R. H. and Goldberg, M. E., editors, *The Neurobiology of Saccadic Eye Movements*, pages 13–67. Elsevier Science Publishers B. V.

Boahen, K. (1997). The retinomorphic approach: Pixel-parallel adaptive amplification, filtering and quantization. *Analog Integ. Circ. and Sig. Proc.*, 13(1/2):53–68.

Carley, L. R. (1989). Trimming analog circuits using floating-gate analog MOS memory. *IEEE J. Solid State Circ.*, 24(6):1569–1575.

Collewijn, H. and Tamminga, E. P. (1984). Human smooth and saccadic eye movements during voluntary pursuit of different target motions on different backgrounds. *J. Physiol.*, 351:217–250.

Collins, C. C., O'Meara, D., and Scott, A. B. (1975). Muscle tension during unrestrained human eye movements. *J. Physiol.*, 245:351–369.

DeWeerth, S. P. (1992). Analog VLSI circuits for stimulus localization and centroid computation. *Intl. J. Comp. Vis.*, 8(3):191–202.

Diorio, C., Hasler, P., Minch, B., and Mead, C. (1997). A complementary pair of four-terminal silicon synapses. *Analog Integ. Circ. and Sig. Proc.*, 13(1/2):153–166.

Diorio, C., Mahajan, S., Hasler, P., Minch, B., and Mead, C. (1995). A high-

resolution non-volatile analog memory cell. In *Proc. of the Intl. Symp. on Circuits and Systems*, pages 2233–2236. Seattle, WA.

Douglas, R., Mahowald, M., and Mead, C. (1995). Neuromorphic analogue VLSI. In Cowan, W. M., Shooter, E. M., Stevens, C. F., and Thompson, R. F., editors, *Annual Reviews in Neuroscience, Vol. 18*, pages 255–281. Annual Reviews Inc., Palo Alto, CA.

Elias, J. G. (1993). Artificial dendritic trees. *Neural Computation*, 5(4):648–664.

Ferrera, V. and Lisberger, S. (1995). Attention and target selection for smooth pursuit eye movements. *J. Neurosci.*, 15(11):7472–7484.

Ferrera, V. and Lisberger, S. (1997). The effect of a moving distractor on the initiation of smooth-pursuit eye movements. *Visual Neuroscience*, 14:323–338.

Fukushima, K., Yamaguchi, Y., Yasuda, M., and Nagata, S. (1970). An electronic model of the retina. *Proc. of the IEEE*, 58:1950–1951.

Glasser, L. A. (1985). A UV write-enabled PROM. In Fuchs, H., editor, *Chapel Hill Conference on VLSI (1985)*, pages 61–65. Computer Science Press, Rockville, MD.

Godaux, E. and Cheron, G. (1996). The hypothesis of the uniqueness of the oculomotor neural integrator - direct experimental evidence in the cat. *J. Physiology London*, 492(2):517–527.

Goldreich, D., Krauzlis, R. J., and Lisberger, S. G. (1992). Effect of changing

feedback delay on spontaneous oscillations in smooth pursuit eye movements of monkeys. *J. Neurophysiol.*, 67(3):625–638.

Groh, J. M., Born, R. T., and Newsome, W. T. (1997). How is a sensory map read out? effects of microstimulation in visual area MT on saccades and smooth pursuit eye movements. *J. Neurosci.*, 17:4312–4330.

Hasler, P., Diorio, C., Minch, B. A., and Mead, C. (1995). Single transistor learning synapses. In Tesauro, G., Touretzky, D., and Leen, T., editors, *Advances in Neural Information Processing Systems 7*, pages 817–824. MIT Press, Cambridge, MA.

Hepp, K., Henn, V., Vilis, T., and Cohen, B. (1989). Brainstem regions related to saccade generation. In Wurtz, R. H. and Goldberg, M. E., editors, *The Neurobiology of Saccadic Eye Movements*, pages 105–212. Elsevier Science Publishers B. V.

Hoffman, J. and Subramaniam, B. (1995). The role of visual attention in saccadic eye movements. *Perception and Psychophysics*, 57(6):787–795.

Horiuchi, T. (1995). An auditory localization and coordinate transform chip. In Tesauro, G., Touretzky, D., and Leen, T., editors, *Advances in Neural Information Processing Systems 7*, pages 787–794. MIT Press, Cambridge, MA.

Horiuchi, T., Bishofberger, B., and Koch, C. (1994). An analog VLSI saccadic system. In Cowan, Tesauro, and Alspector, editors, *Advances in Neural Information Processing Systems 6*, pages 582–589. Morgan Kaufmann, San Mateo, CA.

Horiuchi, T. K. and Koch, C. (1996). Analog VLSI circuits for visual motion-based adaptation of post-saccadic drift. In *Proc. 5th Intl. Conf. on Microelectronics for Neural Networks and Fuzzy Systems - MicroNeuro96*, pages 60–66. Feb. 12-14, 1996, Lausanne, Switzerland, IEEE Computer Society Press, Los Alamitos, CA.

Jürgens, R., Becker, W., and Kornhuber, H. H. (1981). Natural and drug-induced variations of velocity and duration of human saccadic eye movements: Evidence for a control of the neural pulse generator by local feedback. *Biol. Cybern.*, 39:87–96.

Kalayjian, Z. and Andreou, A. (1997). Asynchronous communication of 2D motion information using winner-takes-all arbitration. *Analog Integ. Circ. and Sig. Proc.*, 13(1/2):103–109.

Keller, E. L. (1973). Accomodative vergence in the alert monkey. montor unit analysis. *Vision Res.*, 13:1565–1575.

Kerns, D. A. (1993). *Experiments in Very Large-Scale Analog Computation*. PhD thesis, Electrical Engineering, California Institute of Technology.

Khurana, B. and Kowler, E. (1987). Shared attentional control of smooth eye movement and perception. *Vision Research*, 27(9):1603–1618.

King, W. M., Lisberger, S. G., and Fuchs, A. F. (1986). Oblique saccadic eye movements. *J. Neurophysiol.*, 56:769–784.

Koch, C. (1989). Seeing chips: Analog VLSI circuits for computer vision. *Neural Computation*, 1:184–200.

Koch, C. and Ullman, S. (1985). Shifts in selective visual attention: Towards the underlying neural circuitry. *Human Neurobiology*, 4:219–227.

Kowler, E., Anderson, E., Dosher, B., and Blaser, E. (1995). The role of attention in the programming of saccades. *Vision Research*, 35(13):1897–1916.

Lande, T. S., Ranjbar, H., Ismail, M., and Berg, Y. (1996). An analog floating-gate memory in a standard digital technology. In *Proc. 5th Intl. Conf. on Microelectronics for Neural Networks and Fuzzy Systems - MicroNeuro96*, pages 271–276. Feb. 12-14, 1996, Lausanne, Switzerland, IEEE Computer Society Press, Los Alamitos, CA.

Laughlin, S., van Steveninck, R. R. d., and Anderson, J. C. (1998). The metabolic cost of neural information. *Nature Neurosci.*, 1(1):36–41.

Lisberger, S. G. and Ferrera, V. P. (1997). Vector averaging for smooth pursuit eye movements intitiated by two moving targets in monkeys. *J. Neurosci*, 17(19):7490–7502.

Lisberger, S. G., Morris, E. J., and Tychsen, L. (1987). Visual motion processing and sensory-motor integration for smooth pursuit eye movements. In Cowan, W. M., Shooter, E. M., Stevens, C. F., and Thompson, R. F., editors, *Annual Reviews in Neuroscience, Vol. 10*, pages 97–129. Annual Reviews Inc., Palo Alto, CA.

McKenzie, A. and Lisberger, S. G. (1986). Properties of signals that determine the amplitude and direction of saccadic eye movements in monkeys. *J. Neurophysiol.*, 56(1):196–207.

Mead, C. (1989a). Adaptive retina. In Mead, C. and Ismail, M., editors, *Analog VLSI Implementation of Neural Systems*, pages 239–246. Kluwer Academic Publishers, Boston, MA.

Mead, C. (1989b). *Analog VLSI and Neural Systems*. Addison-Wesley, Menlo Park, CA.

Mead, C. (1990). Neuromorphic electronic systems. *Proc. IEEE*, 78(10):1629–1636.

Morris, E. J. and Lisberger, S. G. (1985). A computer model that predicts monkey smooth pursuit eye movements on a millisecond timescale. *Soc. Neurosci. Abstr.*, 11:79.

Morris, T. G. and DeWeerth, S. P. (1996). Analog VLSI circuits for covert attentional shifts. In *Proc. 5th Intl. Conf. on Microelectronics for Neural Networks and Fuzzy Systems - MicroNeuro96*, pages 30–37. Feb. 12-14, 1996, Lausanne, Switzerland, IEEE Computer Society Press, Los Alamitos, CA.

Mortara, A. (1997). A pulsed communication/computation framework for analog VLSI perceptive systems. *Analog Integ. Circ. and Sig. Proc.*, 13(1/2):93–101.

Nichols, M. J. and Sparks, D. L. (1995). Non-stationary properties of the saccadic system - new constraints on models of saccadic control. *J. Neurophysiol.*, 73(1):431–435.

Niebur, E. and Erdős, P. (1993). Theory of the locomotion of nematodes: control of the somatic motor neurons by interneurons. *Mathematical Biosciences*, 118:51–82.

Optican, L. M. and Miles, F. A. (1985). Visually induced adaptive changes in primate saccadic oculomotor control signals. *J. Neurophysiol.*, 54(4):940–958.

Optican, L. M. and Robinson, D. A. (1980). Cerebellar-dependent adaptive control of the primate saccadic system. *J. Neurophysiol.*, 44:1058–1076.

Rafal, R., Calabresi, P., Brennan, C., and Scioltio, T. (1989). Saccade preparation inhibits reorienting to recently attended locations. *J. Exp. Psych: Hum. Percep. and Perf.*, 15:673–685.

Rashbass, C. (1961). The relationship between saccadic and smooth tracking eye movements. *J. Physiol.*, 159:326–338.

Robinson, D. (1973). Models of the saccadic eye movement control system. *Kybernetik*, 14:71–83.

Robinson, D. A. (1964). The mechanics of human saccadic eye movement. *J. Physiol.*, 174:245–264.

Sarpeshkar, R. (1997). Efficient precise computation with noisy components: extrapolating from electronics to neurobiology. submitted to Neural Computation.

Shimojo, S., Tanaka, Y., Hikosaka, O., and Miyauchi, S. (1995). Vision, attention, and action – inhibition and facilitation in sensory motor links revealed by the

reaction time and the line-motion. In Inui, T. and McClelland, J. L., editors, *Attention and Performance XVI*. MIT Press.

Strassman, A., Highstein, S. M., and McCrea, R. A. (1986). Anatomy and physiology of saccadic burst neurons in the alert squirrel monkey .1. excitatory burst neurons. *J. Comp. Neur.*, 249(3):337–357.

Tam, W. J. and Ono, H. (1994). Fixation disengagement and eye-movement latency. *Perception and Psychophysics*, 56(3):251–260.

Treue, S. and Maunsell, J. (1996). Attentional modulation of visual motion processing in cortical areas MT and MST. *Nature*, 382:539–541.

Watamaniuk, S. N. J. and Heinen, S. J. (1994). Smooth pursuit eye movements to dynamic random-dot stimuli. *Soc. Neuroscience Abstr.*, 20:317.

Westheimer, G. (1954). Mechanism of saccadic eye movements. *Arch. Opthamol.*, 52:710.

Westheimer, G. A. and McKee, S. (1975). Visual acuity in the presence of retinal image motion. *J. Opt. Soc. Am*, 65:847–850.

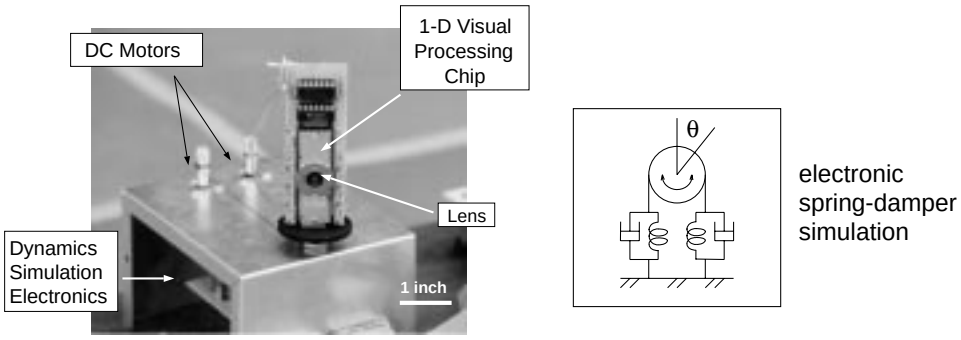

Figure 1: Photograph of the one-dimensional oculomotor plant. Two DC motors pull on both ends of a drive thread wrapped around the circumference of a small turntable. An analog silicon retina (described in section 3) is mounted vertically on the turntable for reduced rotational inertia. A lens is mounted directly onto the face of the chip to focus an image onto the silicon die. An electronic circuit (mounted inside the box) simulates the mechanical dynamics of the primate oculomotor plant, implementing an overdamped spring-mass system.

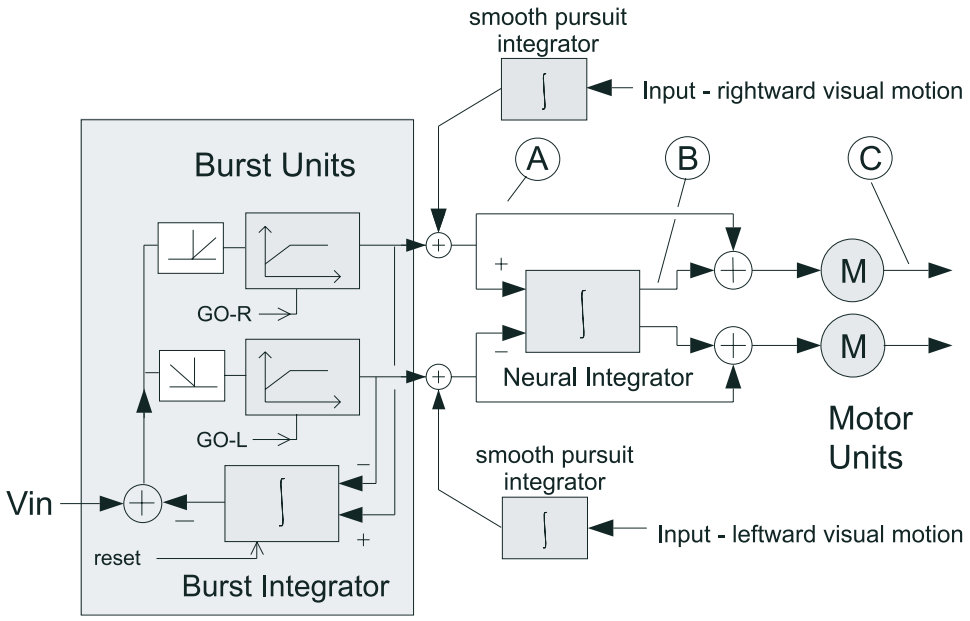

Figure 2: Block diagram of the oculomotor control circuitry. Saccadic eye movements are driven by the burst units to a given displacement determined by the input, Vin, provided by the retinal *location* of the visual target. Smooth pursuit eye movements are driven by the pursuit integrators which output eye velocity commands. The pursuit integrators receive a target's retinal *slip* as their input and provide an eye velocity signal as their output. Eye velocity signals are then integrated to eye position (neural integrator), thereby maintaining a memory of the current eye position. The motor unit outputs are an appropriately weighted combination of the velocity and position signals, given the dynamics of the oculomotor plant. Signals A, B, and C for a saccadic eye movement are shown in Fig. 3A. See text for an explanation of the burst units.

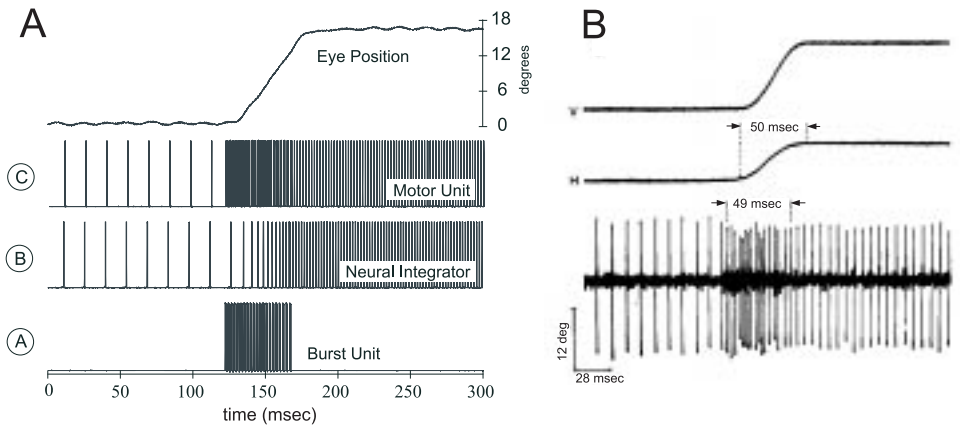

Figure 3: **(A)** : The eye position, burst unit, neural integrator output, and motor unit spike trains during a small saccade. The initial horizontal eye position is off-center with the neural integrator providing the tonic holding activity. All three spike trains are digital outputs (0 to 5 volts). Note that only the motor unit output (C) is used externally. The small oscillation seen in the eye position trace is due to the pulse-frequency modulation technique used to drive the eye. Eye position is measured directly using the potentiometer which doubles as the mechanical bearing for the system. **(B)**: Motor neuron spike train with horizontal (H) and vertical (V) eye position shown during an oblique saccade in a rhesus monkey (From King et al., 1986)

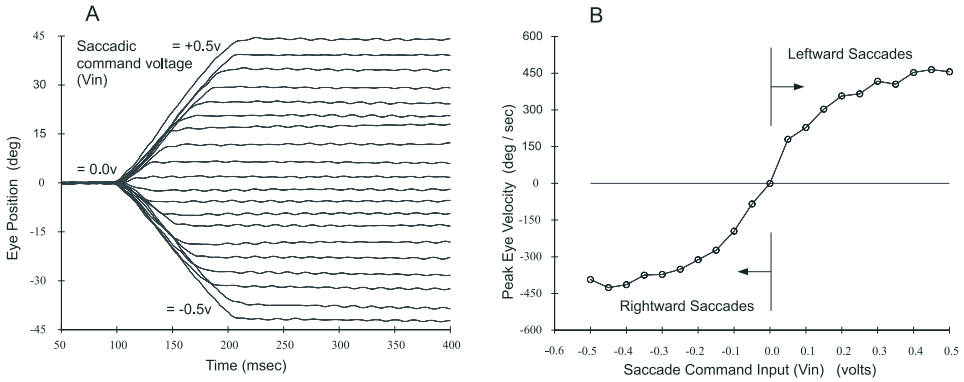

Figure 4: **(A)**: Angular eye position vs. time for 20 traces of different saccades triggered from the center position. The input was swept uniformly for different saccade amplitudes from leftward to rightward. The small oscillations in the eye position are due to the discrete pulses used to drive the eye motors; at rest, the pulses are at their lowest frequency and thus most visible. **(B)**: Plot of the peak velocity during each of the saccades on the left. These velocities were computed by performing a least-squares fit to the slope of the center region of the saccade trace. Peak velocities of up to 870 degrees/sec have been recorded on this system with different parameter settings than used here.

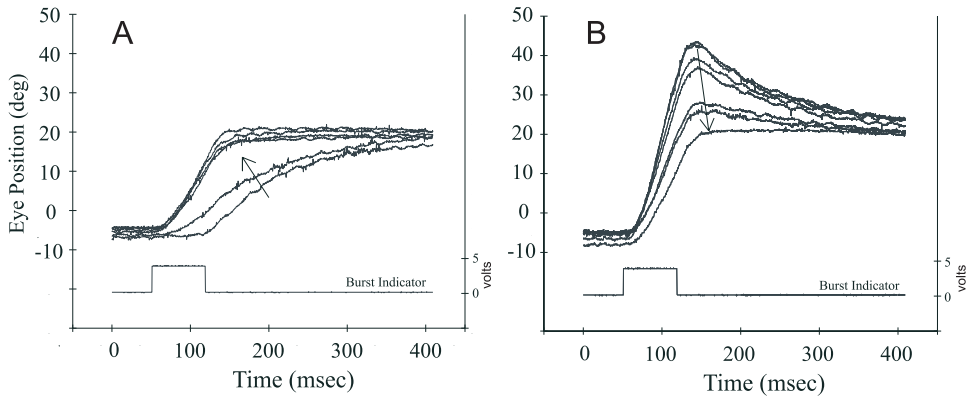

Figure 5: **(A)** Reduction of Saccadic Undershoot via On-chip Learning: saccade trajectories demonstrating the reduction of a backward post-saccadic drift by increasing the burst gain via a tunneling process which modifies the charge stored on a non-volatile floating-gate memory circuit in an unsupervised manner. The circuit converged within 8 practice saccades (not all shown). **(B)** Reduction of Saccadic Overshoot: saccade trajectories showing the reduction of an onward post-saccadic drift by decreasing the burst gain via a hot-electron injection process which modifies the charge on the same memory circuit as above but in the opposite direction. In this case, the performance converged in 41 practice saccades. The lower digital trace in each figure indicates the time of burst unit activity. The arrow indicates the progression from early saccade trials to later saccade trials. The floating-gate technology demonstrated here (Hasler et al., 1995; Diorio et al., 1995) provides us with a versatile, single transistor adaptive synapse.

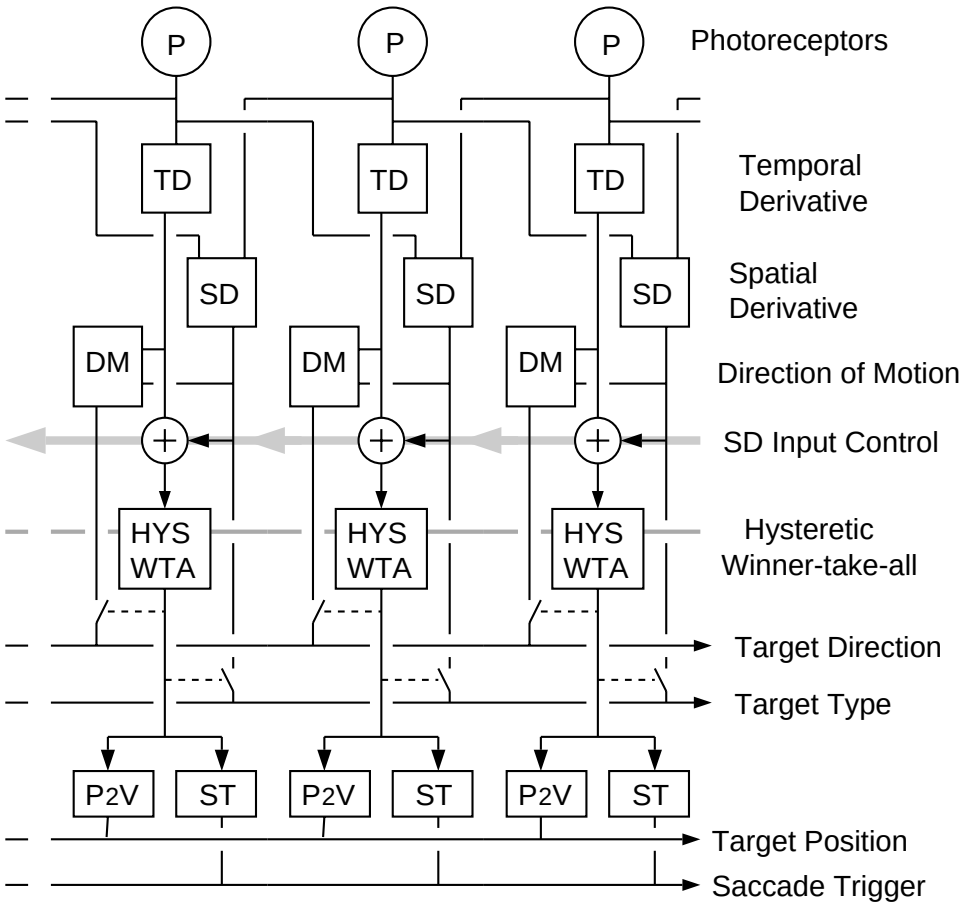

Figure 6: Block Diagram of the Visual Tracking Chip: Images are projected directly onto the chip surface's through a lens and the output signals are sent to the oculomotor plant described in section 2. P = adaptive photoreceptor circuit, TD = temporal derivative circuit, SD = spatial derivative, DM = direction of motion, HYS WTA = hysteretic winner-take-all, P2V = position to voltage, ST = saccade trigger. The TD and SD signals are summed to form the saliency map from which the HYS WTA finds the maximum. Hysteresis is used locally to improve the tracking of moving targets as well as to combat noise. The output of the HYS WTA steers both the direction-of-motion and the SD information onto global output lines. The HYS WTA also drives the P2V and ST circuits to convert the winning position to a voltage and to indicate when the selected pixel is outside a specified window located at the center of the array. The SD input control modulates the relative gain of the positive and negative spatial derivatives used in the saliency map. See the text for details.

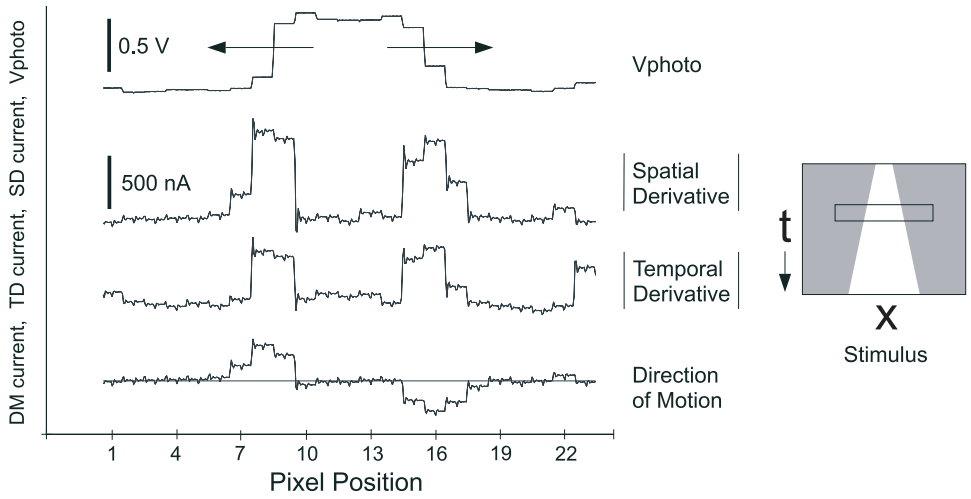

Figure 7: Example stimulus - Traces from top to bottom: Photoreceptor voltage, absolute value of the spatial derivative, absolute value of the temporal derivative, and direction-of-motion. The stimulus is a high-contrast, expanding bar (shown on the right), which provides two edges moving in opposite directions. The signed, temporal and spatial derivative signals are used to compute the direction-of-motion shown in the bottom trace. The three lower traces were current measurements which shows some clocking noise from the scanners used to obtain the data.

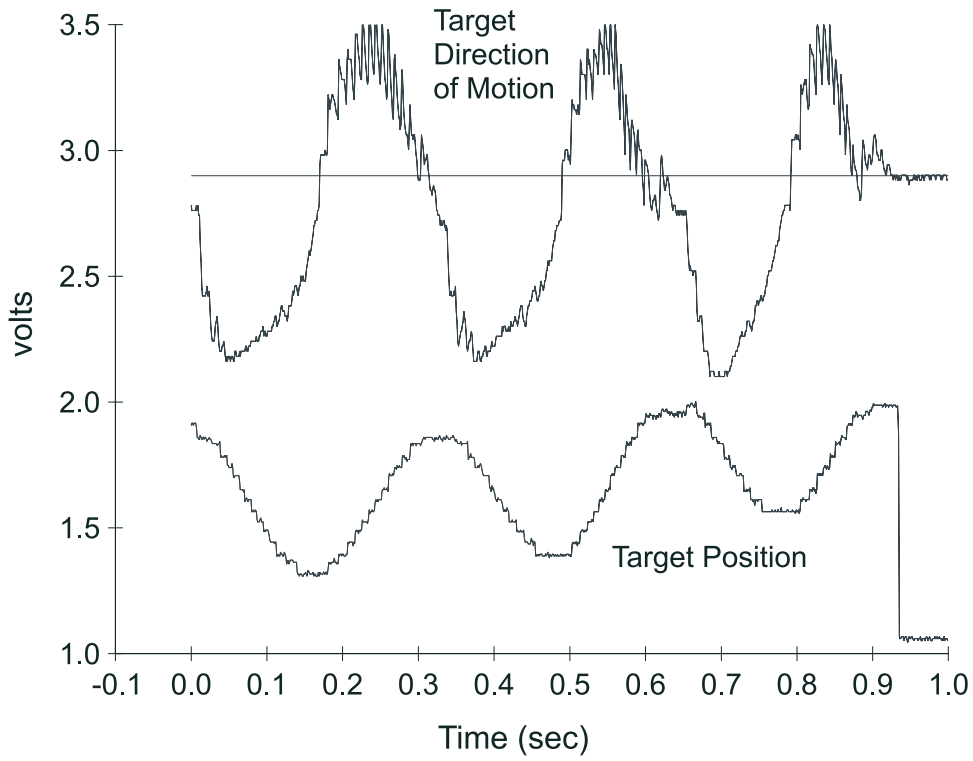

Figure 8: Extracting the target's position and direction of motion from a swinging target: The WTA output voltage is used to switch the DM current onto a common current-sensing line. The output of this signal, converted to a voltage, is seen in the top trace. The zero-motion level is indicated by the flat line shown at 2.9 volts. The lower trace shows the target's position from the position-to-voltage encoding circuits. The target's position and direction of motion are used to drive saccades and smooth pursuit eye movement during tracking. The noise in the upper trace is due to switching transients as WTA circuits switch in the DM currents from different pixel locations.

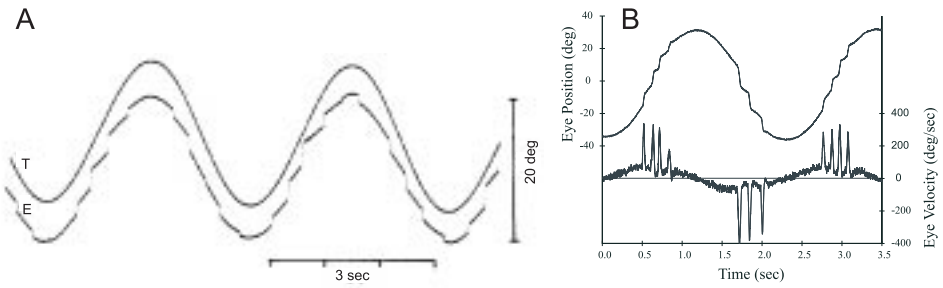

Figure 9: **(A)**: Smooth pursuit and saccadic eye movements of a monkey in response to sinusoidal target motion at approximately 0.27 Hz, peak-to-peak amplitude 20 deg. The target and eye position traces have been offset for clarity (From Collewijn and Tamminga, 1984). **(B)**: Smooth pursuit and saccadic eye movements in our VLSI model. A swinging target consisting of a bar with no distractors is tracked over a few cycles. The top trace shows the eye position over time and the bottom trace shows the eye velocity.

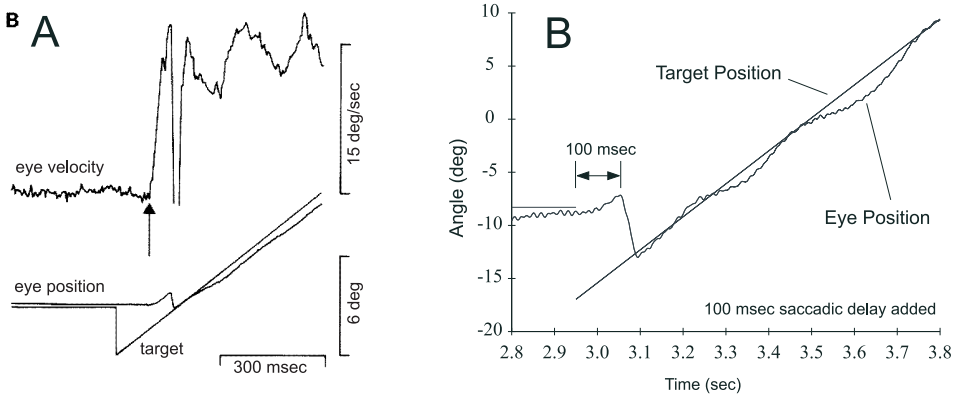

Figure 10: (**A**): Step-Ramp experiment with a macaque monkey: The upward arrow indicates the initiation of pursuit, which precedes the first saccade. (From Lisberger, Morris, and Tychsen, 1987). (**B**): Step-Ramp Experiment using the model: The target jumps from the fixation point to a new location and begins moving with constant velocity. An artificial delay of 100 msec has been added to simulate the saccadic triggering latency. Note: only the saccadic trigger is delayed; the target information is current.